Marine Pollution Bulletin 209 (2024) 117067

Contents lists available at ScienceDirect

Marine Pollution Bulletin

journal homepage: www.elsevier.com/locate/marpolbul

Effects of sea ice on Baltic Sea eutrophication

Ove Parn [c], Olaf Duteil [e], Elisa Garcia-Gorriz [a], Nuno Ferreira-Cordeiro [d], Gennadi Lessin [b], Diego Macias [a], Svetla Miladinova [a], Chiara Piroddi [a], Luca Polimene [a,*], Natalia Serpetti [a], Adolf Stips [a]

[a] European Commission, Joint Research Centre, Via E. Fermi 2749, 21027 Ispra, VA, Italy
[b] Plymouth Marine Laboratory, Prospect Pl, Plymouth PL1 3DH, United Kingdom
[c] EstMare OU, Nelgi 30, Tallinn, Estonia
[d] SEIDOR ITALY SRL, Via Castel Morrone, 20129 Milano, Italy
[e] Duteil Environmental Numerics, Reventloustrasse, 17, 24235 Laboe, Germany

ARTICLE INFO

Keywords:
Eutrophication indicators
Impact of sea ice on eutrophication
Effects of anthropogenic pressure
Trophic transfer index
Dia/Dino index
Baltic sea ecosystem
Nutrient dynamics

ABSTRACT

This study investigates the influence of sea ice on eutrophication in the Baltic Sea ecosystem by comparing simulations from 1953 to 2017, with ice and without ice cover. We assessed the impact from ice cover by using eutrophication indicators defined by the Marine Strategy Framework Directive (MSFD), the Dia/Dino index and the newly proposed Trophic Transfer Index (TTI). Five out of six indicators suggest a negative impact of sea ice on the eutrophication status of the Baltic Sea, with a marked increase in ice impact observed in the early 1970s, followed by a decline in the late 1980s. The linear correlation between ice impact on MSFD indicators and nutrient loads suggests that the influence of ice becomes more pronounced under conditions of elevated nutrient loads. Around 1988, both the TTI and Dia/Dino index indicate eutrophication amplification, with ice cover significantly impacting both indicators (approximately 30 %), leading to a shift towards dinoflagellate dominance. While ice influences plankton timing and ecosystem structure, nutrient loads remain the primary driver of the timing of spring and summer blooms. According to our study the reduction in sea ice cover due to climate change, could contribute to the faster achievement of the Baltic Sea's Good Environmental Status.

1. Introduction

The Baltic Sea is a seasonally ice-covered, semi-enclosed brackish sea with a unique temperate to subarctic climate gradient and is sensitive to global changes. It is affected by various human-induced environmental pressures, including shipping, overfishing, pollution from biological and chemical sources, and marine litter (HELCOM, 2018a). The direct effects of climate change are increased water temperatures, reduced coverage and thickness of sea ice (Haapala et al., 2015; Vihma and Haapala, 2009), and increased amount of precipitation in the northern part of the catchment (Andersson et al., 2015). The indirect effects include altered stratification, increased acidification (Omstedt et al., 2014), biodiversity loss and the spread of non-indigenous species (Ojaveer et al., 2021). The effects of climate change on marine species are multifaceted, with phytoplankton, cyanobacteria, and zooplankton responding differently, while shifts in species interactions and trophic dynamics significantly influence the ecosystem (Viitasalo and Bonsdorff, 2022). Eutrophication further exacerbates these issues, leading to algal blooms, increased turbidity, oxygen depletion, and altered species composition, all of which threaten biodiversity (HELCOM, 2018a, 2021). Despite efforts to reduce nutrient inputs from land, oxygen depletion and the expansion of anoxic areas persist. This is due to the inefficient burial of phosphorus under anoxic conditions, which leads to its release from sediments and perpetuates eutrophication (Kuliński et al., 2022; Meier et al., 2023).

Key abiotic factors, such as light availability for photosynthesis, nutrient concentrations, water temperature, salinity, ocean currents, and sea ice, are all influenced by climate change. Distinguishing between the impacts of climate change and human-induced eutrophication is complex, yet crucial for maintaining a healthy marine ecosystem (Blue Manifesto, 2020). Marine ecosystem models are essential tools for understanding these intricate relationships and developing effective management strategies to mitigate the combined effects of human activities and climate change.

The ecological role and preferred environmental conditions of the

* Corresponding author.
E-mail address: Luca.POLIMENE@ec.europa.eu (L. Polimene).

https://doi.org/10.1016/j.marpolbul.2024.117067
Received 25 June 2024; Received in revised form 26 September 2024; Accepted 26 September 2024
Available online 14 October 2024

phytoplankton are determined based on their size, shape, growth rate and motility. These characteristics dictate the pathway of material and energy into the pelagic and benthic food web. In recent decades, the Baltic Sea's algal spring bloom has frequently exhibited dinoflagellate dominance, particularly in seasonally ice-covered regions (Klais et al., 2011, 2013). The distribution and abundance of diatoms and dinoflagellates significantly influence primary production, forming the foundation of marine food webs. Larger and more nutritious diatoms typically support larger zooplankton populations (Stoecker and Pierson, 2019), whereas dinoflagellates, often smaller and with lower sinking rates, can lead to different trophic pathways. The sedimentation velocity of diatoms is generally higher due to their heavier silica frustules, which affects sedimentation patterns and benthic habitats. Changes in zooplankton communities subsequently impact higher trophic levels, including fish and marine mammals. These complex interactions within the food web ultimately shape the health and productivity of marine ecosystems (Spilling et al., 2018).

The diatom/dinoflagellate (Dia/Dino) index is a pivotal indicator of the composition and dynamics of phytoplankton. Several studies have emphasised the impact of eutrophication on the displacement of the dominance patterns in the phytoplankton spring bloom, using the Dia/Dino index as an indicator of good environmental status (GES) (HELCOM, 2018b; Wasmund, 2017; Wasmund et al., 2017). However, Pärn et al. (2021) demonstrated that the conditions for mixing within euphotic zones are critical drivers of the shift from diatom dominance to dinoflagellate dominance in parts of the Baltic Sea during the spring bloom. Climate change alters the sea ice and wind conditions, affecting these mixing conditions. Additionally, sea ice conditions are strongly correlated with summer chlorophyll-a (chl-a) levels in coastal waters, indicating a substantial role of ice in regulating the summer chl-a levels in the Baltic Sea (Vigouroux et al., 2021).

Light and stratification are key factors that control the phytoplankton spring bloom (Kari et al., 2018). Sea ice affects underwater light conditions by limiting the amount of light transmitted through the surface and modifying the water mixing and nutrient circulation beneath the ice (Katlein et al., 2015). The seasonal ice cover extent plays a crucial role in determining the timing of phytoplankton blooms, which in turn affects the seasonality of ecological processes at Higher Trophic Levels (HTL). Ice cover serves as a major indicator of radical changes in ecological conditions that determine the severity of winter in the Baltic Sea. The mildest winter on record (2019/20) had a maximum ice cover of only 37,000 km^2 (~9 %), while the severest winter (1986/87) recorded an extent of 407,000 km^2 (97 %) (BACC; Author Team, 2015)

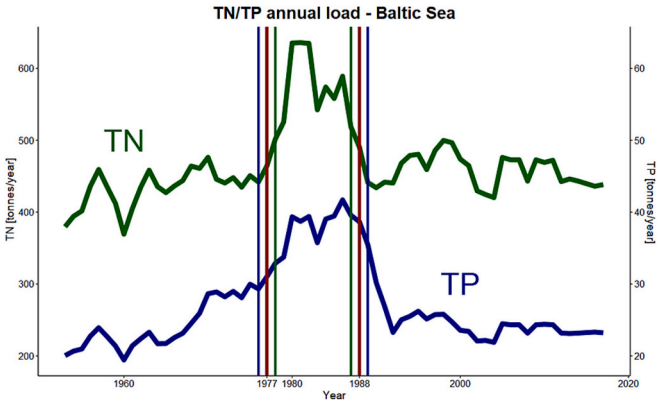

Fig. 1. Riverine nutrient loads into the Baltic Sea (Lessin et al., 2014a). This graph shows annual loads (kt/year) of total nitrogen (TN, green) and total phosphorus (TP, blue) entering the sea via rivers. Blue and green vertical lines indicate TN (1978 and 1987) and TP (1976 and 1989) breakpoints, respectively, and red lines are the mean breakpoints. (For interpretation of the references to colour in this figure legend, the reader is referred to the web version of this article.)

(Fig. 1). Between 1953 and 2017, the Baltic Sea experienced 30 % mild winters and 20 % severe winters. The ice season in the Baltic Sea can extend up to 7 months (Siitam et al., 2017; Vihma and Haapala, 2009), with maximum ice in late February and early March (BACC; Author Team, 2015). Although the melting season begins in March, sea ice can still be observed in the northernmost Bothnian Bay until June (Leppäranta and Myrberg, 2009). The sea ice can reach up to 1.8 m in thickness (Haas, 2004), and due to the ice drift, the ice ridges can measure 5–15 m in thickness (Leppäranta and Myrberg, 2009).

The sea ice profoundly impacts turbulent fluxes at the water surface and beyond, influencing the thermodynamics of the ocean and water mixing. Sea ice and snow cover act as insulators, hindering the exchange of heat, carbon dioxide (CO_2) and other gases between the air and the sea and creating a barrier between the ocean and the atmosphere. Additionally, snow cover on the sea ice significantly affects light distribution. The albedo of freshly fallen snow can be as high as 0.9, whereas that of melting bare ice is only 0.4, but it is markedly higher than that of the open sea (< 0.1) (Vihma and Haapala, 2009). Consequently, a slight reduction in ice or snow cover increases the net solar radiation beneath the water surface.

Diatoms and dinoflagellates are the primary food sources for numerous zooplankton species. The abundance, quality, and diversity of zooplankton rely on the availability of suitable phytoplankton food source. Zooplankton consumes digestible and highly palatable phytoplankton species (Mitra, 2006; Polimene et al., 2015). However, when the dominant phytoplankton are either inedible or less palatable, a significant portion of the carbon synthesised through photosynthesis do not enter in the food chain (Chislock et al., 2013). This leads to an accumulation of phyto detritus and dissolved organic matter in the water column due to non-predatory losses (Eddy et al., 2021), an increase in microbial respiration and a decrease in oxygen levels; these phenomena are typically associated with eutrophication (EEA, 2019). Thus, the effects triggered by enhanced nutrient loads, such as planktonic community composition shifts and feeding behaviour alterations, need to be considered during eutrophication assessment.

Trophic transfer efficiency (TTE) quantifies the effectiveness of carbon transfer across trophic levels (Eddy et al., 2021) and is the conceptual basis for the newly proposed trophic transfer index (TTI) (Polimene et al., 2023). This indicator uses a new approach to assess eutrophication being based on trophic fluxes instead of biogeochemical concentrations (see "methods"). In the present study, we provide, for the first time, a long-term (1957–2017) eutrophication assessment by integrating the TTI with the well-established Marine Strategy Framework Directive (MSFD) eutrophication indicators and the HELCOM pre-core indicator, the Dia/Dino index. The latter, similar to the TTI, captures changes in the quality of primary production and, although based on biomass, provides indirect information on the transfer efficiency between phytoplankton and zooplankton.

Observations of physical, chemical, and biological processes in the Baltic Sea provide crucial data for understanding its complex ecosystem dynamics. Biogeochemical models build upon this knowledge by simulating various scenarios and predicting ecosystem responses to factors such as climate change and nutrient loading. In this study, we utilized the GETM-ERGOM model to examine the impact of sea ice —a key climate change indicator—on the marine ecosystem's capacity to effectively process nutrients. First, we assessed the potential impact of sea ice on marine eutrophication indicators, as defined by the Marine Strategy Framework Directive Descriptor 5. Second, we investigated the influence of sea ice on the shift from diatom prevalence to dinoflagellate dominance in the Baltic Sea using the Dia/Dino index. Third, we employed the TTI to evaluate the effect of sea ice on plankton trophic fluxes. These approaches allow us to explore the intricate interactions within the marine food web and their implications for energy flow and ecosystem health.

2. Materials and methods

2.1. Eutrophication indicators

2.1.1. Marine strategy framework directive (MSFD) indicators

The evaluation of eutrophication employed key indicators specified by MSFD, as described by Ferreira et al. (2011), including concentrations of dissolved inorganic nitrogen (DIN; when applicable to nitrate and ammonium), dissolved inorganic phosphorus (DIP; both indicative of MSFD descriptor D5C1), and chlorophyll-a (chl-a; addressing MSFD descriptor D5C2). Additionally, oxygen concentrations above the bottom were used as a representation of MSFD descriptor D5C5. These descriptors form an integrated approach to assess and manage the effects of eutrophication on marine ecosystems. By monitoring these factors, policymakers and experts can work to prevent and mitigate the negative impacts of eutrophication.

2.1.2. The Dia/dino index

The Dia/Dino index (D4C1 in MSFD), categorized as a pre-core indicator by HELCOM, aligns with the supporting descriptors of the Baltic Marine Environment Protection Commission (Helsinki Commission [HELCOM]; https://indicators.helcom.fi/indicator/diatom-dinoflagellate-index/). HELCOM evaluates progress towards achieving the goal of a "Baltic Sea unaffected by eutrophication," as outlined in the Baltic Sea Action Plan (BSAP). This goal is further described by ecological objectives, including nutrient concentrations close to natural levels, clear waters, natural levels of algal blooms, natural distribution and occurrence of plants and animals, and natural oxygen levels. HELCOM employs indicators with defined numerical threshold values to systematically assess these objectives. The Dia/Dino index, which reflects dominant patterns in the biomass of the spring phytoplankton bloom, relies on values for diatom and dinoflagellate biomass.

The Dia/Dino index reflects the relative dominance of diatoms over dinoflagellates during the spring phytoplankton bloom and provides a proxy for estimating nutrient entry into the pelagic or benthic food web. When diatoms dominate, their rapid sinking diminishes the availability of food for zooplankton but augments the food supply to zoobenthos (HELCOM, 2018b). Alterations in the dominance of diatoms or dinoflagellates impact the dynamics of both pelagic and benthic food webs due to disparities in their quality as food sources and the timing of their occurrence (Wasmund, 2017). A low Dia/Dino index signals potential silicate limitation (Wasmund et al., 2017; HELCOM, 2018b).

The Dia/Dino index (Wasmund, 2017), representing the relative percentage of diatoms, was calculated as follows:

$$\frac{Dia}{Dino}index = \frac{ConcentrationofDiatoms}{ConcentrationofDiatoms + ConcentrationofFlagellates} \quad (1)$$

It was used to compute the spring averages (1 February - 31 May) of phytoplankton concentration in chlorophyll units for the surface layer (0-10 m) based on the model results. Very low phytoplankton concentrations are irrelevant in the calculation of the spring bloom, and small values can introduce errors into the statistical analysis when dividing. Therefore, if the monthly average diatom or dinoflagellate concentration at a grid point was below 0.1 mg/L, these small values were excluded from the Dia/Dino index calculation. The index calculation involved first determining the monthly average phytoplankton values at each grid point, then calculating the average for the surface layer, and finally computing the average across the Baltic Sea.

Diatom dominance, and thus a high Dia/Dino index, are typical in historical data and are therefore assumed to reflect good environmental status (GES) (Wasmund, 2017).

The model conditions under which diatoms or dinoflagellates dominate are detailed in Appendix 1. Sea ice reduces wind-driven turbulence, causing diatoms to sink and influencing phytoplankton composition. Under-ice stratification allows dinoflagellates to stay near the surface due to their neutral buoyancy. Thus, pre-bloom ice conditions affect phytoplankton composition: diatoms sink below the euphotic zone under ice, favoring dinoflagellates, while wind-driven turbulence keeps diatoms suspended, leading them to dominate the spring bloom.

2.1.3. Trophic transfer index

The method assumes that eutrophication impacts a marine area when an increase in primary production is not mirrored by a corresponding increase in grazing activity (Polimene et al., 2023, Tubay et al., 2013). This concept is substantiated by the evidence that eutrophication is triggered by extended periods of un-grazed primary production (Chislock et al., 2013; EEA, 2019; Eddy et al., 2021).

The consequence of this assumption is that, in a healthy environment, and over appropriate timeframes, grazing is correlated to primary production (PP) (Kemp et al., 2001; Schmoker et al., 2013), irrespective of the system's trophic condition. The strength of this correlation is assessed by combining the linear (Pearson) and rank (Spearman) correlation coefficients as follows:

$$TTI = max(RL, RR) \quad (2)$$

where RL is the linear correlation coefficient between monthly depth-integrated primary production (*PP*) and grazing (*Grazing*) both expressed in mmol N m^{-2} $month^{-1}$:

$$RL = corrcoef[PP(t), Grazing(t, t+1)] \quad (3)$$

And *RR* is the rank correlation coefficient between PP and the Grazing to PP ratio:

$$RR = Spearman[PP(t), Grazing(t, t+1) : PP(t)] \quad (4)$$

RR allows the TTI to include monotonic correlations steeper than linear. In both Eqs. (3) and (4) *t* indicates the month(s) over which the fluxes are averaged.

Following Polimene et al. (2023) the TTI was calculated in each model grid point over a period of 5 years and used to identify "problem areas" (or TTI-Eutrophic Zone) based on a single threshold value of 0.7. In other words, where the TTI falls below this threshold, primary production is considered not adequately balanced by a corresponding increase in grazing activity and this indicates the potential onset of dysfunctional phenomena (e.g. organic matter accumulation, anoxia etc.). On the contrary, regions where the TTI is equal to or higher than 0.7 are classified as Unaffected Area by Eutrophication (UAbE) due to a "healthy" balance between primary production and grazing.

It should be noted that here we have slightly changed the original formulation proposed in Polimene et al. (2023) by averaging the grazing flux over two months (i.e. t and t + 1, see Eqs. (3) and (4)). We found that with this minor amendment the index is more reliable, giving more realistic results. Furthermore, this approach makes the TTI more generally usable since it accounts for possible mismatch between phytoplankton and grazers due to physiological constraints e.g. low growth rate of the latter with respect to the former. This can be particularly important for biogeochemical models (e.g. ERSEM, Butenschön et al., 2016) explicitly considering relatively slow-growing mesozooplankton (e.g. Roman et al., 2001).

2.1.4. Analysis of the effects of sea ice and nutrient loads

To quantify the 'ice impact' on marine eutrophication indicators [dissolved inorganic nitrogen (DIN), dissolved inorganic phosphorus (DIP), oxygen (O_2), chl-a, Dia/Dino index and TTI], relative differences were computed between two scenarios: without ice ('no ice') and with sea ice as the reference ('ice'). The average values in the model grid were calculated for the following depths: chl-a and the Dia/Dino index were averaged over the 0–10 m depth range, while DIN and DIP were averaged over the entire water column, from the surface to the bottom.

To track temporal changes, we calculated spatial averages for each indicator in both scenarios on a monthly basis. We then determined the

temporal average over the simulation period and assessed the impact of ice using the formula (ice − no_ice) / ice × 100. Annual averages were computed from monthly averages for all indicators except the Dia/Dino index, which was based on data from February 1 to May 31.

We computed the monthly average for each indicator at each grid point for both scenarios to estimate spatial differences. Subsequently, we derived annual or longer-term averages from these monthly data.

In order to evaluate the outcomes of the model scenarios, we compared the 'ice impact' to determine the increase or decrease in the selected eutrophication indicator under the no-ice scenario. Notably, the model's ice calculation was robust and might have underestimated the extent of ice (Pärn et al., 2021).

The model took into account land-based runoff and nutrient loads which had been incorporated into 20 major rivers (Neumann and Schernewski, 2008). To assess the human impact on marine eutrophication indicators, we calculated the breakpoints using a technique commonly used for change point detection (Zeileis et al., 2003). In Fig. 1, the blue and green vertical lines represent the breakpoints identified for total nitrogen (TN) in 1978 and 1987 and total phosphorus (TP) in 1976 and 1989, respectively. Based on the breakpoints, we divided the time series into three phases: 1: low nutrient load, 1953–1977; 2: high nutrient load, 1978–1988; 3: restored low nutrient load 1989–2017.

Analysis of variance (ANOVA) and Tukey's HSD tests (refer to Supplementary Material S3) identified a statistically significant difference between phases 2 and 1 as well as between 2 and 3, for both TN and TP. However, no statistically significant difference was detected between phases 1 and 3. This finding suggested that in the model experiment, nutrient loads decreased to levels characteristic of the pre-eutrophication, low-productivity phase (Tomczak et al., 2022).

2.2. Model description and set-up

The model simulations utilized a three-dimensional hydrodynamic model, GETM (General Estuarine Transport Model; https://getm.eu/) (Burchard and Bolding, 2002; Stips et al., 2004), coupled to a biogeochemical model, ERGOM (Ecological Regional Ocean Model; www.ergom.net), integrated within FABM (the Framework for Aquatic Biogeochemical Models) (Bruggeman and Bolding, 2014). The ERGOM model version applied in this study included three functional groups of phytoplankton: diatoms, dinoflagellates, and cyanobacteria; a bulk zooplankton group; nitrate, ammonium, and phosphate nutrients; dissolved oxygen; pelagic and benthic detritus; and iron-bound phosphorus in sediments and water. The initial model setup was developed and utilized according to Lessin et al. (2014a, 2014b) and has been thoroughly assessed and validated (Pärn et al., 2020). This model has also been employed in a marine model ensemble study, where its results were found to be in close agreement with those of other similar models (Friedland et al., 2021).

The model domain encompassed the entire Baltic Sea area, with an open boundary in northern Kattegat. The EMODnet bathymetry data (Fig. 1) were interpolated to a model grid with a horizontal resolution of 2 × 2 nm. Twenty-five σ layers were utilized in the vertical (Lessin et al., 2014b). Initial distributions of water temperature and salinity were interpolated to the model grid from monthly climatological data. The model was then subjected to a 7-year spin-up phase. Salinity and temperature distributions at the open boundary were interpolated using monthly climatological data. Initial conditions for typical concentrations of biogeochemical variables were uniformly prescribed within the model domain. Initial oxygen, phosphate, and nitrate are based on data from the World Ocean Database (Garcia et al., 2019).

The default dinoflagellate maximum growth rate in the model is set to 0.4 d^{-1}, and the maximum growth rate for diatoms is 1.3 d^{-1}. When estimating chl-a concentration, the modeled values align with observed data. However, in more detailed comparisons to observations, it is noted that diatom concentration is overestimated, and flagellate concentration is underestimated (Pärn et al., 2021). Spilling (2007) points out that the maximum growth rate for diatoms ranges from 0.6 to 1.2 d^{-1}. In the study by Spilling and Markager (2008), it is shown that common spring diatoms grow at a rate of 0.3–0.7 d^{-1} at 4.5 °C. For this reason, the maximum growth rate of diatoms has been changed in the model to 1.1 d^{-1}. Supplementary material Table S2 presents the parameters used in the ERGOM model for this study, detailing the various inputs and settings that were applied to simulate ecosystem dynamics.

Three-hourly meteorological forcing data (ERA5) obtained from the European Centre for Medium-Range Weather Forecasts (http://www.ecmwf.int) were applied. The model considered land-based runoff and nutrient loads (Fig. 1), including 20 major rivers (Lessin et al., 2014a) with an N:P ratio between 13 and 27.

GETM includes only a thermodynamic sea-ice model, neglecting sea-ice dynamics. To assess the influence of sea ice (Pärn et al., 2022) on indicators, the JRC GETM-ERGOM Framework (Macias et al., 2018) was used to simulate the following scenarios:

- Simulation with sea ice (the 'ice simulation' as the reference).
- Simulation without sea ice. In this scenario, referred to as the 'no ice simulation', sea ice is absent, and no constraints related to sea ice are applied.

In the presence of ice:

- Wind stress within the corresponding grid cell was set to 0.
- The impact of shortwave radiation on a water column decreases when the albedo is 0.3. Light conditions change under sea ice, PARi = 0.7 × PAR, where PAR is photosynthetically active radiation, and PARi is PAR under ice.
- The heat flux from the atmosphere is adjusted to account for the ice reflection (albedo values: 0.85 for snow, 0.6 for ice, and 0.3 for melting ice).

According to model sensitivity test simulations (Supplementary Material S1), the reduction in wind stress caused by sea ice exerts a more pronounced influence on the spring blooms of diatoms and dinoflagellates than the light limitation imposed by the ice, given the model parameters used (Table S2).

3. Results

3.1. Impact of sea ice on MSFD eutrophication indicators

The current findings demonstrate the significant impact of sea ice on eutrophication indicators in the Baltic Sea ecosystem. The extent of sea ice varies annually; the smallest average was in February 2007, with only 6 % coverage of the Baltic Sea, while the largest was in February 1987 at 43 % (Figs. 2 and 3). Although 'maximum ice extent' is a commonly used term to describe sea ice, this indicator differs from the model-calculated ice extent. The model output represents February mean calculations (Fig. 3). Nevertheless, the Pearson's correlation coefficient between maximum ice extent (obtained from the Swedish Meteorological and Hydrological Institute) and model data was 0.92. The ice seasons of 1956, 1963, 1966, 1970, 1979, 1982, 1985, 1986, 1987, 1994, 1996, 2003, 2010, and 2011 are classified as severe (Rjazin et al., 2017).

Sea ice affects the temperature and salinity stratification of the Baltic Sea by weakening wind-induced mixing and altering circulation in different water layers. Simulations reveal a slight increase in mean salinity (0.4 %) under ice-free conditions and a 0.5 % rise in temperature under ice, attributed to the insulating effect of ice (Supplementary Material S4). The mean temperature of the upper 10 m water layer was 7.5 °C (SD = 0.6), with a corresponding salinity of 7.9 PSU (SD = 0.3). Linear regression analysis indicated a trend of 0.02 °C/year for surface temperature and − 0.01 PSU/year for salinity.

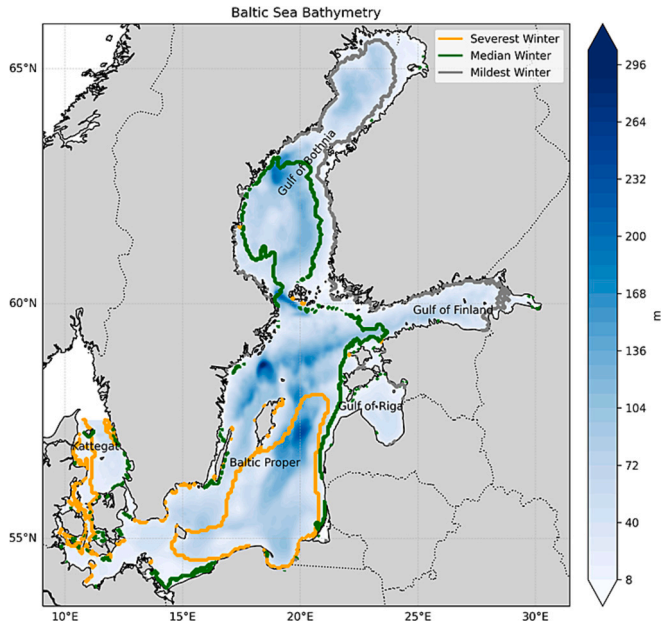

Fig. 2. Bottom topography of the Baltic Sea used in the ocean model. The extent of ice cover during the mildest (grey line), median (green line) and severest (orange line) winter. The sea ice extent is based on the digitised Baltic ice charts (CEMS, 2024). (For interpretation of the references to colour in this figure legend, the reader is referred to the web version of this article.)

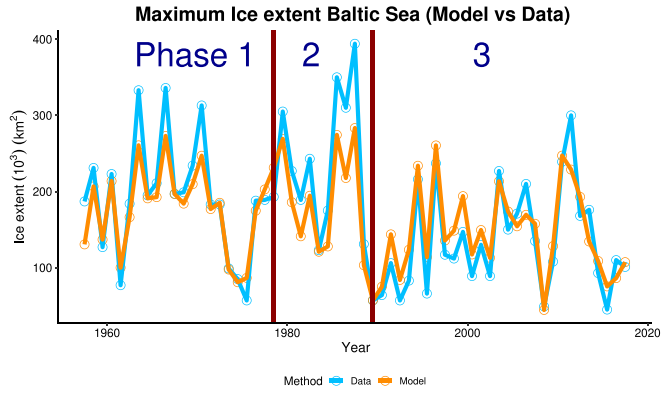

Fig. 3. Average February sea ice extent (1953–2017) from model simulations, compared with observed maximum ice extent (CEMS, 2024). Based on maximum ice extent, severe ice winters exhibit a minimum ice extent of 270,000 km^2.

3.1.1. DIN concentrations (D5C1)

Average DIN concentrations across the Baltic Sea from the surface to the bottom showed a sustained increase from 1953 to 1970 in simulations with ice (Fig. 4), while this increasing trend persisted until 1975 in simulations without ice. This indicates that the system's reaction to the driving factors—referred to here as the 'response time'—was delayed by 5 years in the ice-free simulation compared to the ice-covered one. After this period, the continuously increasing trend abruptly shifted towards a rapid decline. The average concentration of DIN in simulations with ice cover was 5 % lower than in simulations without ice for the period 1953–2017 (Table 1).

To assess the effects of nutrient loads, we analyzed the average indicator values for phases 1, 2, and 3 (p2.1.4), as outlined in Table 2, using nutrient breakpoint detection from 1953 to 2017 (p2.3). ANOVA showed that TN and TP loads did not differ significantly between phases 1 and 3. Therefore, we can conclude that since 1989, the nutrient load to the Baltic Sea in the model has returned to its initial level, as phase 3 resembles phase 1. However, if nutrient load were the sole driver of the indicators presented in Table 2, we would expect phase 3 (average DIN = 3.3 mmol/m^3) to also resemble phase 1 (average DIN = 5.61 mmol/m^3). Nevertheless, ANOVA revealed (Supplementary Material, Fig. S3.1) phase 3 with respect to DIN concentration displays statistically significant differences in indicators compared to phase 1. Thus, it can be inferred that DIN concentration does not follow the restored low nutrient load phases, as phase 3 diverges from phases 1 and 2. The initial state of DIN fails to recover in accordance with nutrient phases. During phase 3, a linear growth rate of 0.06 mmol/m^3 per year was noted in the ice simulation. Nonetheless, the ice impact on DIN does not significantly differ between phases 1 and 3 ($p < 0.01$), indicating that the influence of ice on DIN concentration aligns with the nutrient phases. Ice extent was greatest in phase 1 and was only 78 % of this extent in phase 3 (Table 2). The ice impact on DIN concentrations was 0.1 % (with a SD of ±7 %) in phase 1, −10.5 % (±6 %) in phase 2, and − 6 % (±7 %) in phase 3.

Furthermore, a significant linear correlation ($p = 0.01$) was established between the ice impact on DIN and nutrient loads, with correlation coefficients of −0.7 for TP and −0.5 for TN.

The spatial distribution of the ice impact on DIN concentrations in the Baltic Sea (Fig. 5) has been visualised over three phases. The first is characterized by near-zero or slightly positive ice impact across the Baltic Sea (Fig. 5), while the shallower areas, such as the Gulfs of Bothnia, Finland and Riga displayed higher values of ice impact compared to the deeper Baltic Proper.

During 1968–1996, the ice impact transitioned to negative or near-zero values, especially in the Baltic Proper, where ice cover reached up to 60 % in some years. The most recent period (1997–2017) witnessed an ice impact pattern mirroring the seafloor topography (Fig. 1). In addition, monthly variations with negative or near-zero ice impact prevailed in deeper marine areas from January to April, while coastal areas experienced negative ice impact during May and June.

3.2. DIP concentrations (D5C1)

In the ice simulation, average DIP concentrations across the Baltic Sea, from the surface to the bottom, remained below 0.5 mmol/m^3 from 1953 to 1968, then increased rapidly starting in 1970 (Fig. 4). In contrast, in the no-ice simulation, the average DIP concentration stayed below 0.5 mmol/m^3 until 1987, after which it increased rapidly, 16 years later than in the ice simulation. Notably, the increase in DIP concentration in the no-ice simulation occurred during a period of marked decrease in nutrient load into the sea (Fig. 1), reaching its third phase as detailed in Table 2. During phase 3, a linear growth rate of 0.04 mmol/m^3 per year was recorded in the ice simulation.

ANOVA revealed a statistically significant difference between the timeseries of DIP concentration with and without ice, indicating that the ice impact is statistically significant. Additionally, phases 1 to 3, which assess anthropogenic impact, are statistically different. Therefore, the DIP concentration does not follow the nutrient load phases. However, the impact of ice on DIP during phases 1 and 3 did not show any statistically significant difference ($p < 0.01$). Thus, it can be deduced that the influence of ice on DIP concentration statistically aligns with the nutrient phases.

Moreover, a significant correlation was established between the ice impact on DIP and nutrient loads ($p = 0.01$), with linear correlation coefficients of 0.86 for TP and 0.8 for TN.

Spatially, the effect of ice on DIP concentration is generally uniform across the region. However, from 1953 to 1968, the Gulf of Finland experienced a significantly greater impact from ice compared to the average. In contrast, from 1969 to 1991 and from 1992 to 2017, the ice impact on DIP in the Gulf of Finland was no longer above average. Instead, a negative ice impact on DIP concentrations has emerged in the deeper northern parts of the Baltic Sea (Fig. 5). From 1953 to 1968, the ice impact on DIP concentration remained below 7 %, with a mean of 4

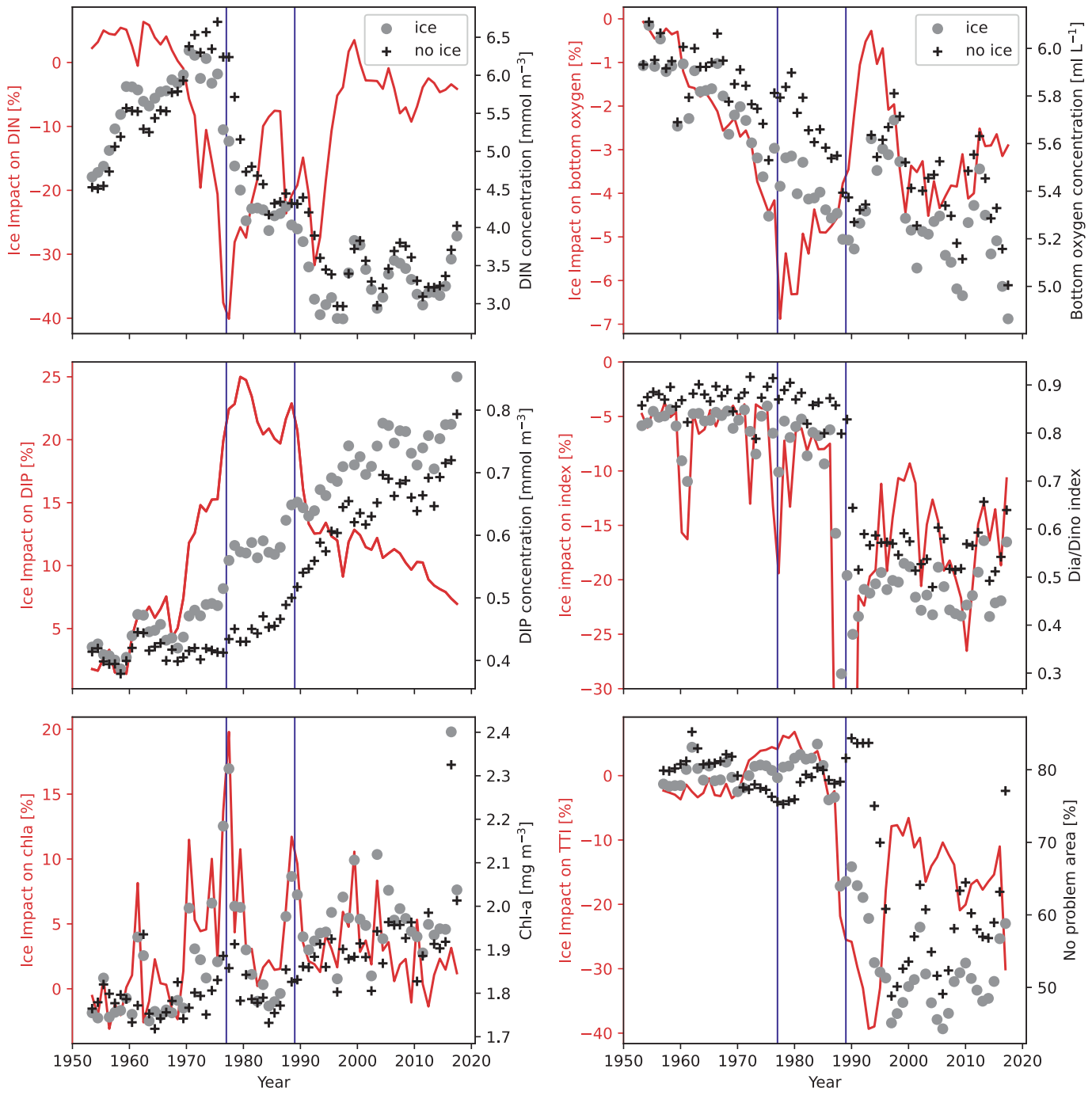

Fig. 4. The ice impact and average concentration of indicators over the Baltic Sea. The red line represents the ice impact, while black dots show simulation results with sea ice, and '+' symbols show results without sea ice. A blue vertical line marks the boundary between Phases 1, 2, and 3. (For interpretation of the references to colour in this figure legend, the reader is referred to the web version of this article.)

%, while it was consistently high at 2 %–28 % (mean 20 %) in the subsequent phase from 1969 to 1991.

3.3. Chl-a concentration (D5C2)

Chl-a concentration serves as a parameter to estimate photosynthetic biomass, encompassing diatoms, dinoflagellates, and cyanobacteria. While the average chl-a concentrations in the surface layer (0–10 m) of the Baltic Sea showed a small but steady rise from 1953 to 2017 (Fig. 4, Table 3), no linear correlation was found between nutrient loads and average chl-a concentrations.

The chl-a concentrations in phases 1, 2, and 3 did not differ statistically significantly, indicating that chl-a concentrations are not responding to the nutrient load phases. During phase 3, a linear growth rate of 0.01 mg/m^3 per year was in the ice simulation. However, a significant correlation ($p = 0.01$) was established between the ice impact on chl-a and nutrient loads, with linear correlation coefficients of 0.65 for TP and 0.42 for TN, indicating that the ice impact follows the nutrient load phases.

The ice impact was negative on the Gulf of Riga, Gulf of Finland, and the northern part of the Gulf of Bothnia (Fig. 5, chl-a) from 1953 to 1969, indicating lower phytoplankton biomass in the presence of sea ice. However, after 1970, the ice impact on chl-a concentration was predominantly positive in the Gulf of Finland, the Baltic Proper, and the

Table 1
Effects of ice cover on eutrophication indicators: mean (and SD) indicator values in simulations with and without ice for the periods 1953–2017.

Variable	ICE	NO_ICE	ICE_IMPACT
DIN (mmol/l)	4.2 (1.1)	4.5 (1)	−5 (8)
DIP (mmol/l)	0.6 (0.1)	0.52 (0.1)	12 (6)
CHL (mg/l)	1.9 (0.13)	1.8 (0.09)	3.2 (4)
O2 (ml/l)	5.45 (0.2)	5.6 (0.2)	−3 (1.6)
Dia/dino	0.62 (0.18)	0.71 (0.16)	−16 (21)
% of Unaffected Area by Eutrophication According to TTI	70 (14)	75 (12)	−7.5 (9)

Table 2
Nutrient loads and their effects on indicators: mean (and SD) values for phases identified by breakpoint detection: 1: low nutrient load, 1953–1977; 2: high nutrient load, 1978–1988; 3: restored low nutrient load 1989–2017.

Variable	Phase 1	Phase 2	Phase 3
TP (t/year)	24,470 (3870)	38,030 (2300)	25,150 (1710)
TN (t/year)	434,220 (29600)	564,120 (63400)	458,490 (22100)
DIN_ice (mmol/m^3)	5.61 (0.49)	4.2 (0.15)	3.3 (0.32)
DIP_ice (mmol/m^3)	0.45 (0.04)	0.59 (0.03)	0.72 (0.05)
CHL_ice (mg/m^3)	1.85 (0.1)	1.89 (0.1)	1.98 (0.1)
O2_ice (ml/l)	5.7 (0.19)	5.4 (0.1)	5.2 (0.2)
% of Unaffected Area by Eutrophication According to TTI	82 (2)	81 (4)	55 (7)
Ice extent (km^2)	8186 (2342)	7866 (3332)	6438 (2430)
Ice_impact_DIN (%)	0.01 (7)	−10.5 (6)	−4.02 (7)
Ice_impact_DIP (%)	8.02 (6)	22.10 (1.8)	11.64 (2.7)
ice_imp_chl (%)	2.78 (5.7)	4.19 (3.8)	3.36 (2.7)
ice_impact_o2 (%)	−2.2 (1.6)	−5.1 (0.7)	−2.9 (1.2)

Kattegat. In the Gulf of Riga, the negative ice impact persisted from 1969 to 1991. From 1992 to 2017, the average ice impact was close to zero, which does not imply the absence of ice impact. Areas covered by ice every winter (Fig. 2, grey line) exhibited a negative ice impact, while a positive impact was detected in the southern part of the sea (Fig. 5, chl-a).

3.4. Bottom O2 concentrations (D5C5)

The current study found that mean bottom O_2 concentrations were consistently lower (by 1 %–7 %) in the ice simulation compared to the no-ice simulation. In the ice simulation, bottom O_2 concentrations began to decline in 1973 (Fig. 4), while in the no-ice simulation, the decline continued for an additional eight years, with O_2 levels remaining stable until 1981. The bottom O_2 concentration in the Baltic Sea largely depends on inflows of highly saline waters (Lehmann et al., 2022), but sea ice lowered the average oxygen concentration by 3 %.

The concentration of O_2 decreased across phases 1, 2, and 3 (Table 2). Therefore, the reduction in nutrient load during phase 3 did not lead to an increase in O_2 concentrations. Instead, during phase 3, a linear decline rate of −0.02 ml/l per year was observed in the ice simulation. The linear correlation between the ice impact on bottom oxygen and nutrient loads was significant ($p = 0.01$), with linear correlation coefficients of 0.67 for TP and 0.68 for TN, suggests that the ice impact on O_2 concentration increases with higher nutrient loads.

In areas with strong water column mixing, oxygen levels are stable and similar in both ice-covered and ice-free conditions (Supplementary Material Fig. S5). However, in deeper regions with naturally lower oxygen levels, sea ice can worsen hypoxia, with oxygen concentrations being over 20 % higher in ice-free simulations. An exception is in the northern Baltic Sea, where ice formation can paradoxically increase deep-water oxygen levels (Fig. S5).

3.5. Effect of sea ice on the Dia/Dino index in the Baltic Sea

The time-averaged Dia/Dino index for simulations with and without ice was 0.62 and 0.71, respectively, from 1953 to 2017 (Table 1), with an ANOVA test indicating statistically significant differences in the time series. The ice impact on the index over this period was −16 %. In regions covered by sea ice, the diatom-to-dinoflagellate ratio remained stable yearly. The average index value for ice areas throughout the study period was 0.5, with the highest value observed at 0.53 and the lowest at 0.48 in 1978. According to the model, ice-covered regions exhibit a slight dominance of dinoflagellates each spring.

At the beginning of the simulation period, the Dia/Dino index value was 0.65–0.8 with the ice simulation and >0.8 without the ice simulation until spring 1987 (Fig. 4). The average concentration of dinoflagellates in the Baltic Sea was low, with diatom dominance. However, ice cover affected the diatom-to-dinoflagellate ratio. The Dia/Dino index with the ice simulation was significantly correlated (−0.76) with the mean ice extent from 1953 to 1986 (Fig. 4, Dia/Dino).

In the sea ice simulation, there is an average 15 % dominance of dinoflagellates over diatoms in the upper 10 m layer of the sea. Since ice reduces surface layer mixing, heavier diatoms sink to the seafloor (Supplementary material S1). This leads to long-term impacts on eutrophication, resulting in 4–5 % more organic matter accumulating in the seabed in the ice-covered simulation compared to the ice-free simulation.

The simulation with sea ice in the model significantly decreased the index value in 1987, marking the beginning of eutrophication (HELCOM, 2018b, Wasmund, 2017 and Fig. S1.4). The modeled time series of the Dia/Dino index (Fig. 4, Dia/Dino) shows a similar pattern to the index calculated from measurements (HELCOM, 2018b), with a dramatic drop in the index value in 1987. The 1986/87 winter witnessed the highest ice coverage throughout the entire study period, reaching a maximum extent of 97 % in the Baltic Sea, while in spring, the index with ice dropped to 0.3, and the ice impact was −140 %. Concurrently, a high ice impact was observed on other indicators (Fig. 4). After a sharp decline, the index began to rise again. During phase 3, a linear growth rate of 0.02 per year was observed in the ice simulation.

3.6. The impact of sea ice and nutrient loads on TTI

The Trophic Transfer Index (TTI) reflects favorable marine conditions in the Baltic Sea from 1953 to 1987, with the Unaffected Area by Eutrophication (UAbE) comprising 80 % of the sea (Fig. 4) in simulations that include sea ice. In 1988, however, the UAbE experienced a substantial decline of 60 % in the ice-covered simulation, whereas it expanded to 85 % in the simulation without ice. Starting in 1993, both simulations showed a 50 % decrease in the UAbE.

According to the TTI, the onset of eutrophication in the Baltic Sea began in 1988 in the ice-covered simulation. Notably, 1987 recorded the most extensive sea ice coverage during the study period. Paradoxically, nutrient loads decreased during this time but coincided with the beginning of phase 3 (Table 2). In non-eutrophied phases, the ice impact was relatively low, at −0.3 % in phase 1 and +0.5 % in phase 2. The average impact of ice in phase 3 was −9 %. After a sharp decline, the UAbE began to increase again. During phase 3, a linear growth rate of 315 km^2 per year was recorded in the ice simulation.

In the ice simulation from 1953 to 2017, the mean phytoplankton-to-zooplankton ratio was 7.4 in the UAbE (SD = 1) and 7.8 in the TTI-eutrophic zone (SD = 1.3), indicating a 5.4 % lower effectiveness of carbon transfer across trophic levels in the TTI-eutrophic zone compared to the UAbE. In the simulation without ice, the phytoplankton-to-zooplankton ratio was 6.9 (SD = 0.3) in the UAbE and 7.6 (SD = 0.7) in the TTI-eutrophic zone, resulting in a 10 % lower effectiveness in the TTI-eutrophic zone compared to the UAbE. The year-average standard

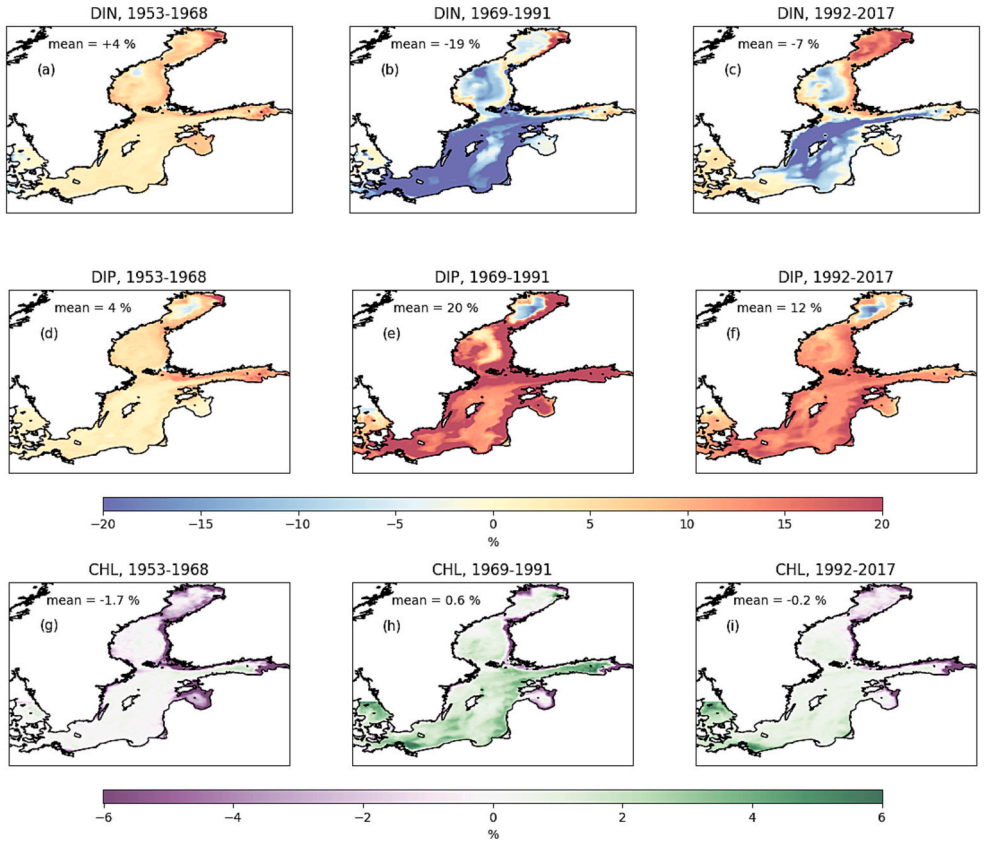

Fig. 5. Ice impact in %.

Table 3
Mean percentage difference in parameters between the Unaffected Area by Eutrophication (UAbE) and the TTI-Eutrophic Zone (simulation with and without ice cover). Phyto/zoo represents trophic energy transfer.

	Phase	DIP (%)		DIN (%)		Pyto/zoo (%)
	ice	No ice	ice	No ice	ice	No ice
1	8	1	−3	−23	−7.8	−6.7
2	−15	−4	−10	−35	−0.3	−11.6
3	−240	7	−163	−1	−11	−12

deviation of the phytoplankton-to-zooplankton ratio was more than twice as small in the simulation without ice compared to the simulation with ice, indicating greater fluctuations in this variable with sea ice simulation and demonstrating a higher sensitivity of trophic transfer compared to the simulation without ice.

To assess the impact of human activity on the Trophic Transfer Index (TTI), we analyzed indicators across phases 1–3. The mean difference in the phytoplankton-to-zooplankton ratio between the UAbE and the TTI-eutrophic zone ranged from −0.3 % to −12 % across these phases 1–3 (Table 3). The concentrations of DIN and DIP exhibited significant variation. At the beginning of the study, during phase 1 (ice simulation), the distribution of DIN and DIP between the UAbE and the TTI-eutrophic zone differed by <15 %. However, beginning in 1988, during phase 3, the TTI-eutrophic zone displayed DIP and DIN levels that were 240 % and 163 % higher than the UAbE, respectively (Table 3).

We analyzed how sea ice affects Trophic Transfer Index (TTI) values (Fig. 6a, b, c) across phases 1–3 by comparing the TTI values (Eq. (4)) in simulations with and without ice. Positive index values indicate that sea ice enhances energy transfer, while negative values suggest higher energy transfer in simulations without ice. During phase 1 (Fig. 6a-c, green), sea ice increased TTI values in shallow coastal areas, the Bothnian Bay, the Gulf of Finland, and the Gulf of Riga. In a large portion of the study area, the ice impact on TTI values was negligible. During phase 2, the effect of ice was much stronger; ice increased energy transfer in coastal areas, the Bothnian Bay, the Gulf of Finland, the Gulf of Riga, as well as the eastern coast of the Baltic Proper and the Kattegat area. The ice impact was significantly negative (Fig. 6a-c purple) in the deep parts of the sea. During phase 3, the effect of ice on the TTI values was positive only in the shallow Bothnian Bay. Everywhere else, energy transfer was higher in the simulation without ice.

3.6.1. The role of ice and nutrient loading in Baltic Sea trophic interactions

The model results differentiate between the effects of changes in ice extent and nutrient load. Ice cover influences the timing of blooms, but the most substantial changes occur during periods of high nutrient load (phase 2). This suggests that nutrient enrichment may enhance the ice impact on spring and summer blooms.

We calculated monthly primary production (PP) values for the Baltic Sea and identified the month with the highest value in the first half of the year, which we refer to as the spring maximum. Similarly, we identified the month with the highest value in the second half of the year as the summer maximum.

In simulations with ice (Fig. 7), the spring PP maximum occurred every year (100 %) in April during low nutrient load, phase 1. In contrast, in simulations without ice, the maxima occurred in April 92 % of the time, with 8 % shifting to March. During phase 2, with ice, 67 % of PP maxima occurred in April, and 33 % shifted to March. Without ice, 64 % of PP maxima occurred in April, and 36 % in March. This indicates a shift of over 33 % in the timing of the maxima from April to March between phases 1 and 2. However, the ice impact on the timing of the maxima is <8 %. Comparing phases 1 and 3, there was a 10 % shift in PP maxima from April to March. This means that in 10 % of the years, the PP maximum values occurred less frequently in April, indicating that the spring bloom happened one month earlier in those years.

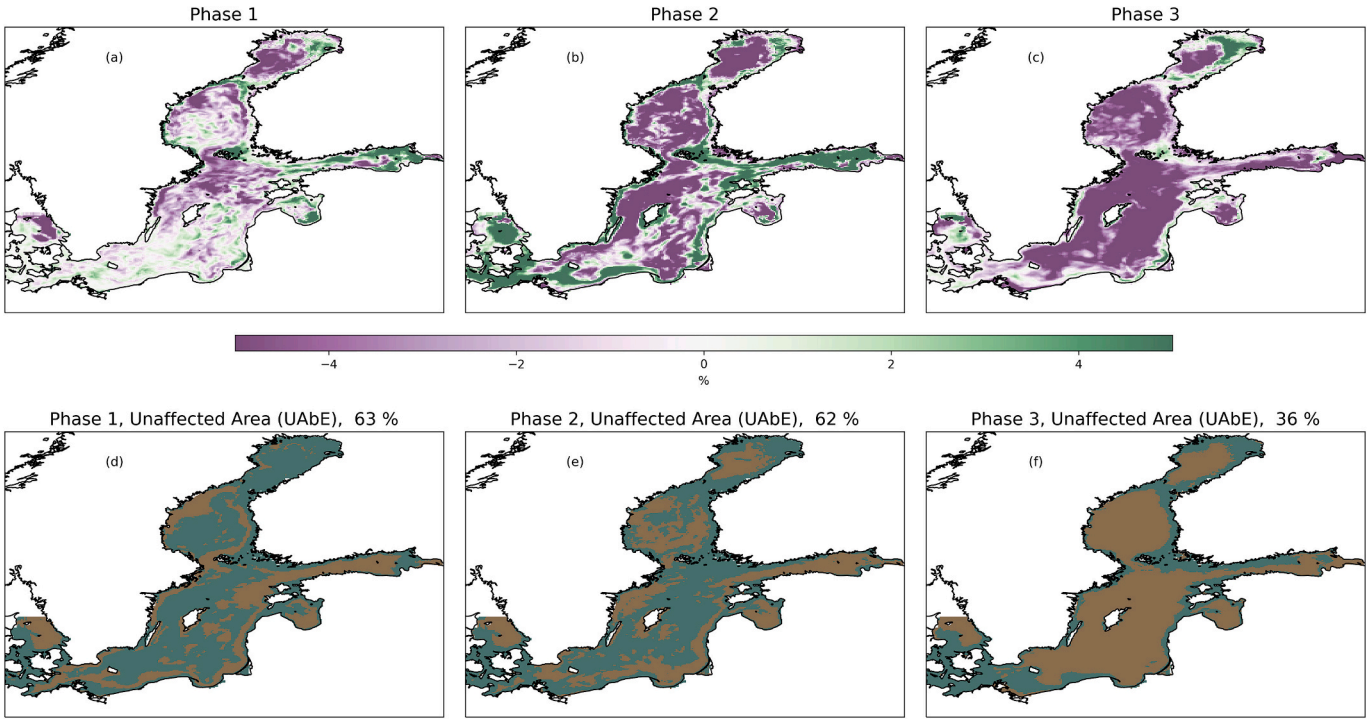

Fig. 6. (a), (b), and (c) indicate the ice impact of TTI in phases 1, 2, and 3. (d)-(f) show the TTI-Eutrophic Zone and Unaffected Area by Eutrophication (UAbE), with brown indicating eutrophic areas and green indicating Unaffected Areas. (For interpretation of the references to colour in this figure legend, the reader is referred to the web version of this article.)

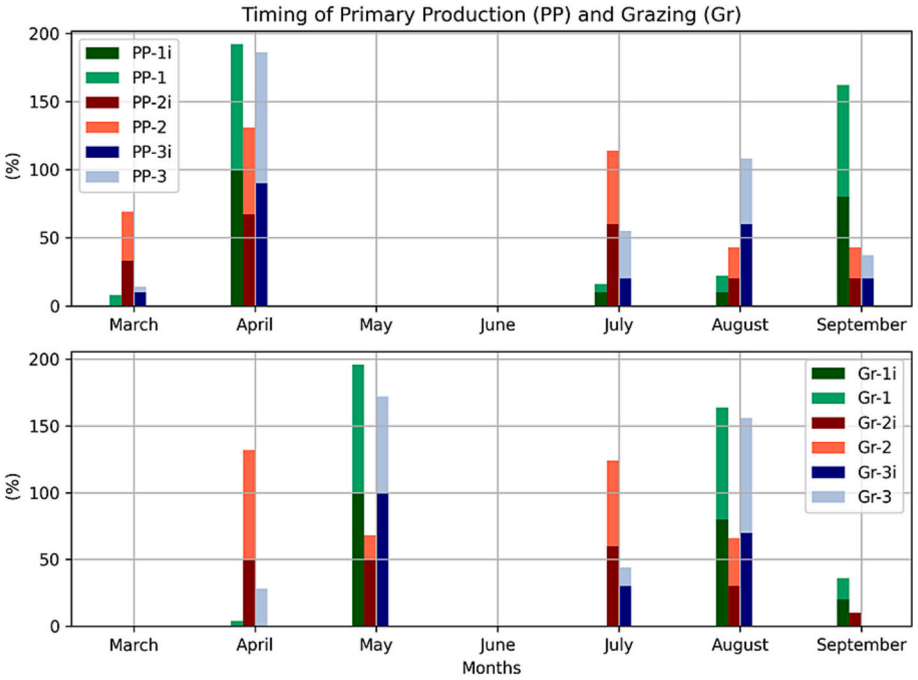

Fig. 7. Timing of Peak Primary Production (PP) and Grazing (Gr) Concentrations in Periods 1–3. PP-1i and PP-1: The low nutrient load period (Period 1) is represented by dark green and light green for ice and no ice simulations, respectively; PP-2i and PP-2: The high nutrient load period (Period 2) is represented by dark red and red; PP-3i and PP-3: The restored low nutrient load period (Period 3) is represented by dark blue and light blue. (For interpretation of the references to colour in this figure legend, the reader is referred to the web version of this article.)

During phase 3, 90 % of PP maxima occurred in April and 10 % in March with ice, while 96 % occurred in April and 4 % in March without ice. This suggests that nutrient overload leads to a larger shift in PP timing, while ice has a smaller influence.

The timing of PP (Fig. 7) and zooplankton grazing (Gr max) varies across phases 1, 2, and 3, with sea ice affecting these processes differently. In a healthy ocean ecosystem, zooplankton grazing typically increases as plankton blooms become more abundant. However, the timing of these events has shifted over time, causing plankton blooms to peak at different times than the peak of grazing activity by zooplankton.

This phase lag between PP and Gr impacts the efficient energy flow through the food web, as measured by the Trophic Transfer Index (TTI). Therefore, the timing of PP and Gr affects the TTI analysis results (Pärn et al., 2024; Supplementary Material Fig. S6).

4. Discussion

The Baltic Sea is subject to considerable anthropogenic pressures, with eutrophication being a primary concern. Despite extensive efforts to mitigate nutrient loads, the ecosystem's recovery has been sluggish (Elmgren et al., 2015), resulting in persistent deep-water anoxia and recurring cyanobacterial blooms (Reckermann et al., 2022). Eutrophication is driven not only by excessive nutrient inputs but also by climate change (Meier et al., 2022), complicating the assessment of its spatio-temporal dynamics. Understanding these interactions is vital for devising sustainable management strategies.

This study explores the Baltic Sea ecosystem's dynamics by analyzing eutrophication indicators in relation to sea ice cover and nutrient loads. External nutrient loads serve as the initial source driving eutrophication. Through changepoint detection applied to nutrient load data, three distinct phases were identified: 1, low (1953–1977); 2, high (1978–1988), and 3, restored low (1989–2017). This segmentation facilitates a detailed examination of trends before and after changes in nutrient loads, underscoring the impact of anthropogenic activities on marine eutrophication. The term "ice impact" describes the influence of ice on the ecosystem, particularly through reductions in light availability and diminished wind-induced surface layer mixing. The model does not account for the direct interactions between algae and sea ice, such as processes involving diatoms enclosed within the ice, phytoplankton attached beneath the ice, or ice-derived algae.

Ecosystem models, such as the JRC GETM-ERGOM Framework, are crucial for understanding complex ecological processes and informing management decisions. However, these models have limitations, including the simplification of biogeochemical processes and the generalization of phytoplankton species into broad categories like diatoms, dinoflagellates, and cyanobacteria. This simplification may obscure the diverse responses of individual species to environmental changes, potentially introducing inaccuracies into predictions. Additionally, the limited spatial and temporal resolution of these models constrains their ability to capture fine-scale patterns and short-term processes, essential for understanding localized and rapid ecological changes. The accuracy of model outcomes also depends on the precision of parameters and input data, which may carry uncertainties.

The simulation results demonstrate that changes in hydrodynamic conditions, such as stratification, water mixing, and currents, driven by the presence of sea ice, significantly impact phytoplankton biomass distribution. Dinoflagellates benefit from reduced turbulence under sea ice, as their buoyancy allows them to remain in the nutrient-rich upper layers of the water column, providing a competitive advantage in maintaining access to light and nutrients. In contrast, diatoms, being non-motile and heavier, tend to sink rapidly under these low-turbulence conditions. However, during ice-free periods (no-ice simulation), stronger vertical mixing counteracts the effects of gravity, suspending diatoms in the upper layers. This allows diatoms to thrive during the spring bloom, where their faster growth rate enables them to outcompete dinoflagellates. Consequently, simulations with ice cover show a 15 % increase in the dominance of dinoflagellates over diatoms in the upper 10 m of the water column. This shift in dominance also impacts the nutrient dynamics, as dinoflagellates are 2.75 times less efficient at nutrient uptake compared to diatoms (Table S2).

This resulted in a 4–5 % increase in organic matter accumulation on the seabed, leading to long-term negative effects on eutrophication. In the bottom layers, simulation results showed that chlorophyll-a concentrations were, on average, 5 % higher in ice scenarios, and cyanobacteria concentrations were 25 % higher. The decomposition of cyanobacteria consumes oxygen, potentially leading to hypoxia in deeper waters. During this decomposition process, nitrogen and phosphorus are released back into the water column, further fueling eutrophication. Sensitivity tests confirmed (Supplementary Material S1) that reduced turbulence under ice was a more significant factor than light limitation for the observed changes in the diatom-dinoflagellate index, underscoring the broader impact of sea ice on phytoplankton community structure.

The Dia/Dino index from ice simulations exhibited a significant negative linear correlation (−0.76) with mean ice extent from 1953 to 1987. During this period, the index consistently remained above 0.65 in both ice-covered and ice-free simulations, indicating minimal eutrophication. The average ice impact was 3 % (SD = 2). However, from 1988 to 2017, the correlation with mean ice extent diminished, and the Dia/Dino index values fluctuated between 0.3 and 0.7, indicating potential eutrophication. During this period, the average ice impact was 24 % (SD = 30). This substantial shift, consistent with trends described by Wasmund, 2017 (supplementary material S1.4), indicates that changes in the Dia/Dino index cannot be solely attributed to ice-induced hydrodynamic conditions. Notably, the index continued to decline even in ice-free simulations, though the decrease observed five years later, in 1992, was smaller than in the ice simulations. The average Dia/Dino index was 0.6 (indicating no eutrophication) in the no-ice simulation and 0.48 (indicating eutrophication) in the ice simulation during Phase 3. This suggests that the regime shift is primarily driven by the release of nutrients accumulated in the sea, with ice amplifying these effects. The ice impact was seven times greater during Phase 3 compared to the previous phase, indicating that sea ice's influence is significantly enhanced during a eutrophicated phase. Climate warming does not appear to be the direct cause of this shift, as the average spring sea surface temperatures preceding phase 3 (in 1986, 1987, and 1988) did not exceed the phase 2 average.

The timing of trophic interactions between primary production (PP) and grazing within the food web has also shifted. In Phase 1, characterized by low nutrient loads, peak PP consistently occurred in April each spring, while peak grazing was observed in May (in simulations with ice). However, in the restored low nutrient load phase (Phase 3, Fig. 7), peak PP shifted to March in 15 % of the years, although no corresponding shift in grazing timing was observed in ice simulations. In contrast, during the high nutrient load phase, peak PP shifted from April to March in 33 % of the years, while peak grazing timing moved from May to April in 50 % of the years.

Whether this shift in bloom timing is related to climate change remains uncertain due to conflicting evidence. On one hand, a warming trend in sea surface temperature (Zalewska et al., 2024) suggests that water temperatures have increased. For example, the date of reaching the 5.6 °C threshold in the Baltic Sea has shifted earlier by an average of one week across all regions (Pärn et al., 2021). However, satellite-based data on the timing of chlorophyll-a peaks do not correlate with sea surface temperature data (Pärn et al., 2021). Given that the most significant shifts in timing occurred during the high nutrient load (phase 2), it suggests that the primary stressor during this period was the elevated nutrient loads rather than changes in temperature. This indicates that eutrophication is driven by multistressor (nutrient loads, ice, climate change) perturbations rather than a single factor.

According to the TTI, eutrophication began in 1987, with an ice impact of 25 %. This timing aligns with the onset observed through the Dia/Dino index. Both integral indicators reflecting the dynamics of eutrophication exhibit a similar temporal progression. At the start of phase 3, there is a notable decline, followed by a period of improvement. The linear growth trend is 0.02 per year for the Dia/Dino index, while the Unaffected Area by Eutrophication (UAbE) increases by 315 km^2 per year. However, all other indicators suggest a slight deterioration during phase 3, despite the restored low nutrient load phase.

Simulations revealed that, based on all indicators, sea ice plays a crucial role in influencing the ecosystem. Out of six indicators, five demonstrated a negative impact on eutrophication, with DIN being the

only exception, showing a positive effect. From 1953 to 2017, simulations with and without sea ice showed average impacts of 15 % on dissolved inorganic nitrogen (DIN), 8 % on dissolved inorganic phosphorus (DIP), 9 % on chlorophyll-a (chl-a), and −3 % on oxygen (O_2). In comparison, Friedland et al. (2021) found that reductions in total nitrogen (TN) and total phosphorus (TP) of 9 % and 10 %, respectively, were several times smaller than the average ice impact on Marine Strategy Framework Directive (MSFD) indicators.

In the presence of ice, dissolved inorganic nitrogen (DIN) concentrations showed a sustained increase from 1953 to 1970, followed by a decrease. In comparison, simulations without ice showed a delayed decrease in DIN concentrations by five years. The pattern of average dissolved inorganic phosphorus (DIP) concentration in simulations without ice was similar to that in simulations with ice. However, in the ice simulation, the mean DIP concentration remained below 0.5 mmol/m^3 from 1953 to 1968, with a rapid increase beginning in 1970. Conversely, in the no-ice simulation, the mean concentration remained below 5 mmol/m^3 until 1987, followed by a rapid increase 16 years later than in the ice simulation. TTI demonstrated that the eutrophic area expanded in 1988 in simulations with ice, while simulations without ice showed a five-year delay, with the eutrophic area expanding in 1993.

The findings suggest that the ice impact on the MSFD indicators is amplified under nutrient enrichment conditions. Sea ice reduces DIN concentrations, exerting a positive effect on eutrophication, but increases DIP concentrations. The ice impact on chlorophyll-a (Chl-a) concentration was predominantly negative between 1953 and 1969, indicating that sea ice helped to reduce eutrophication during this period. However, from 1970 onwards, this impact shifted to become positive, thus enhancing eutrophication. The effect of sea ice varied across different nutrient load phases. During the phase with low nutrient loads, the ice impact on chl-a was relatively modest, at 2.8 %. This effect became 1.5 times stronger during Phase 2, further enhancing eutrophication, and then weakened slightly, being 1.2 times stronger than in the initial phase. This pattern suggests that the ice impact closely follows changes in nutrient loads (Fig. 4).

Tomczak et al. (2021) refer to the period up to the early 1970s as the "low production phase" or reference ecosystem phase, characterized by well-oxygenated deep waters. In model experiments during this phase, the average oxygen concentration in the bottom layer was approximately 6 ml/l, and the ice impact was minimal, with an average influence of −1.2 %. However, in the last decade, the average oxygen concentration in the bottom layer declined to 4.5 ml/l (ice simulation), with some deeper regions experiencing complete oxygen depletion (0 ml/l). The onset of anoxia at the seabed transforms sediments into active sources of ammonium and phosphorus, as observed by Carstensen et al. (2014). These anoxia-driven nutrient releases exacerbate the eutrophication process.

Despite significant reductions in land-based nutrient loads since the 1980s, the nutrient content of the Baltic Sea has remained steady or slightly increased (DIP) since the 2000s. This persistence is attributed to the historical accumulation of nutrients in the water column and sediments, which have long residence times—5-9 years for nitrogen and 11–49 years for phosphorus (Savchuk, 2018; Gustafsson et al., 2017). These residence times delay the impact of changes in nutrient inputs on water quality, making it challenging to correlate reductions in nutrient loads with immediate improvements in nutrient concentrations. Phosphorus, in particular, has a slower turnover rate due to its tendency to bind with sediments, resulting in a more prolonged response in water column concentrations.

The Baltic Sea's DIP concentration has continued to rise slightly, while the average oxygen concentration in the bottom layer has shown a decreasing trend from 1953 to 2017. This is explained by Stigebrandt and Andersson (2020), who demonstrated that the "pump" of eutrophication in the Baltic Sea lies in the internal phosphorus source (IPS) from anoxic bottoms, which release phosphorus from sediments into the water column. To eliminate the IPS, ecosystem management must mitigate the impact of human activities, specifically nutrient inputs from agriculture and wastewater, to prevent increased phosphorus availability and the onset of anoxic conditions. However, a model experiment revealed that both DIP and bottom oxygen concentrations are also influenced by sea ice, with sea ice having a significant impact—up to 25 % on DIP and 3 % on oxygen levels.

The study's findings suggest that the reduction in sea ice extent due to climate change may contribute to the achievement of the Baltic Sea's Good Environmental Status. This multi-index approach allows for a comprehensive assessment of eutrophication and its effects on the marine ecosystem. However, it is important to note that the study did not account for many phenomena associated with climate change, such as changes in precipitation and temperature. Nonetheless, we can consider the potential impacts of rising temperatures. Warmer temperatures (Gröger et al., 2021) may lead to increased stratification (Hordoir and Meier, 2012) in the water column, reducing vertical mixing and limiting nutrient transport from deeper layers to surface waters, which could decrease algal blooms. However, as sea ice extent and duration decrease (Gröger et al., 2021), reduced nutrient levels in the surface layer and increased turbulent mixing, as suggested by this study, could favour diatom dominance and potentially reduce the later-stage proliferation of cyanobacteria. This would lead to more efficient trophic transfer, with primary production being more fully consumed, resulting in less organic matter settling to the seabed and contributing positively to the reduction of eutrophication.

Conversely, enhanced stratification can exacerbate hypoxic zone formation, potentially increasing internal phosphorus loading from sediments, a process known as internal eutrophication (IPS). According to the study's findings, sea ice reduced oxygen concentrations in the near-bottom layers, suggesting that the decline in ice cover could mitigate or compensate for some negative effects of warming, including hypoxia. Thus, the reduction of sea ice might counterbalance or offset some of the impacts of climate warming.

5. Conclusion

This study demonstrates that sea ice cover significantly influences eutrophication dynamics in the Baltic Sea.

The linear correlation between ice impact on DIN, DIP, chl-a, and O_2 concentrations and nutrient loads indicates that the influence of ice becomes more pronounced under conditions of elevated nutrient loads. By analyzing three distinct periods (1: low nutrient loads, 1953–1977; 2: high nutrient loads, 1978–1988; 3: restored low nutrient loads, 1989–2017), the study demonstrates that the ice impact aligns with changes in nutrient load phases. However, it is important to note that the concentrations of eutrophication indicators do not strictly follow these patterns.

The Trophic Transfer Index (TTI) and dia/dino index both signal the onset of eutrophication around 1988 in ice simulations. During this time, ice cover exerted a substantial influence, exceeding 25 %. Concurrently, the dia/dino index sharply declined (from >0.7 to ~0.5), indicating a shift towards dinoflagellate dominance in the spring phytoplankton community. Despite this decline, both indices displayed linear growth trends afterward, with the dia/dino index increasing by 0.02 per year and the Unaffected Area by Eutrophication (UAbE) expanding by 315 km^2 annually. However, other indicators suggest a slight deterioration during phase 3, despite restored low nutrient loads.

Sea ice affects the timing of plankton blooms and zooplankton grazing, which in turn impacts the TTI and shapes the Baltic Sea's energy flow and trophic structure. This effect was more pronounced during periods of high nutrient loads, suggesting that sea ice's regulatory role may be amplified under nutrient-rich conditions. Ultimately, nutrient loads, rather than sea ice dynamics or climate change, are the primary drivers behind shifts in the timing of spring and summer blooms.

While the immediate benefits of nutrient reduction may not always be evident, reducing nutrient inputs remains essential for mitigating the

long-term adverse effects of climate change.

CRediT authorship contribution statement

Ove Parn: Writing – original draft, Software, Methodology, Investigation, Formal analysis, Data curation, Conceptualization. **Olaf Duteil:** Writing – review & editing, Conceptualization. **Elisa Garcia-Gorriz:** Supervision, Software, Data curation, Conceptualization. **Nuno Ferreira-Cordeiro:** Software, Conceptualization. **Gennadi Lessin:** Writing – review & editing, Supervision, Methodology, Conceptualization. **Diego Macias:** Writing – review & editing, Supervision, Resources, Project administration, Funding acquisition, Conceptualization. **Svetla Miladinova:** Writing – review & editing, Supervision, Software, Conceptualization. **Chiara Piroddi:** Writing – review & editing, Conceptualization. **Luca Polimene:** Writing – review & editing, Supervision, Methodology, Formal analysis, Conceptualization. **Natalia Serpetti:** Writing – review & editing, Conceptualization. **Adolf Stips:** Writing – review & editing, Supervision, Software, Methodology, Investigation, Formal analysis, Data curation, Conceptualization.

Declaration of competing interest

The authors declare that they have no known competing financial interests or personal relationships that could have appeared to influence the work reported in this paper.

Data availability

Data will be made available on request.

Appendix A. Supplementary data

Supplementary data to this article can be found online at https://doi.org/10.1016/j.marpolbul.2024.117067.

References

Andersson, A., Meier, H.M., Ripszam, M., Rowe, O., Wikner, J., Haglund, P., Eilola, K., Legrand, C., Figueroa, D., Paczkowska, J., Lindehoff, E., 2015. Projected future climate change and Baltic Sea ecosystem management. Ambio 44, 345–356. https://doi.org/10.1007/s13280-014-0606-0.

BACC, Author Team, 2015. Second Assessment of Climate Change for the Baltic Sea Basin. In: Regional Climate Studies. Springer Verlag, Berlin, Heidelberg, pp. 145–153.

Blue Manifesto, 2020. The road map to a healthy ocean in 2030. https://www.bluemanifesto.eu/ (34.06.2024).

Bruggeman, J., Bolding, K., 2014. A general framework for aquatic biogeochemical models. Environ. Model. Software 61, 249–265. https://doi.org/10.1016/j.envsoft.2014.04.002.

Burchard, H., Bolding, K., 2002. GETM: A General Estuarine Transport Model. Scientific Documentation. JRC EUR Report 20253EN.

Butenschön, M., Clark, J., Aldridge, J.N., Allen, J.I., Artioli, Y., Blackford, J., Bruggeman, J., Cazenave, P., Ciavatta, S., Kay, S., Lessin, G., 2016. ERSEM 15.06: a generic model for marine biogeochemistry and the ecosystem dynamics of the lower trophic levels. Geosci. Model. Dev. 9 (4).

Carstensen, J., Andersen, J.H., Gustafsson, B.G., Conley, D.J., 2014. Deoxygenation of the Baltic Sea during the last century. Proc. Natl. Acad. Sci. 111 (15), 5628–5633. https://doi.org/10.1073/pnas.1323156111.

Chislock, M.F., Doster, E., Zitomer, R.A., Wilson, A.E., 2013. Eutrophication: causes, consequences, and controls in aquatic ecosystems. Nat. Educ. Knowl. 4 (4), 10.

Eddy, T.D., Bernhardt, J.R., Blanchard, J.L., Cheung, W.W.L., Collèter, M., du Pontavice, H., Fulton, E.A., Gascuel, D., et al., 2021. Energy flow through marine ecosystems: confronting transfer efficiency. Trends Ecol. Evol. 36, 76–86. https://doi.org/10.1016/j.tree.2020.09.006.

EEA, 2019. Nutrient Enrichment and Eutrophication in Europe's Seas: Moving towards a Healthy Marine Environment. Publication Office of the European Union, Luxembourg (Report No 14/2019).

Elmgren, R., Blenckner, T., Andersson, A., 2015. Baltic Sea management: successes and failures. Ambio 44, 335–344. https://doi.org/10.1007/s13280-015-0653-9.

Ferreira, J.G., Andersen, J.H., Borja, A., Bricker, S.B., Camp, J., Da Silva, M.C., Garcés, E., Heiskanen, A.S., Humborg, C., Ignatiades, L., Lancelot, C., 2011. Overview of eutrophication indicators to assess environmental status within the European marine strategy framework directive. Estuar. Coast. Shelf Sci. 93, 117–131. https://doi.org/10.1016/j.ecss.2011.03.014.

Friedland, R., Macias, D., Cossarini, G., Daewel, U., Estournel, C., Garcia-Gorriz, E., Kay, S., Kerimoglu, O., Lazzari, P., Lenhart, H., Moll, A., Pätsch, J., Piroddi, C., Ruardij, P., Samuelsen, A., Stips, A., Tiessen, M., 2021. Effects of nutrient management scenarios on marine eutrophication indicators: a Pan-European, multi-model assessment in support of the marine strategy framework directive. Front. Mar. Sci. 8, 596126. https://doi.org/10.3389/fmars.2021.596126.

Garcia, H.E., Weathers, K.W., Paver, C.R., Smolyar, I., Boyer, T.P., Locarnini, M.M., Zweng, M.M., Mishonov, A.V., Baranova, O.K., Seidov, D., 2019. World ocean atlas 2018. Dissolved inorganic nutrients (phosphate, nitrate and nitrate+ nitrite, silicate) 4.

Gröger, M., Dieterich, C., Haapala, J., Ho-Hagemann, H.T.M., Hagemann, S., Jakacki, J., May, W., Meier, H.E.M., Miller, P.A., Rutgersson, A., Wu, L., 2021. Coupled regional Earth system modeling in the Baltic Sea region. Earth Syst. Dynam. 12, 939–973. https://doi.org/10.5194/esd-12-939-2021.

Gustafsson, E., Savchuk, O.P., Gustafsson, B.G., Müller-Karulis, B., 2017. Key processes in the coupled carbon, nitrogen, and phosphorus cycling of the Baltic Sea. Biogeochemistry 134, 301–317. https://doi.org/10.1007/s10533-017-0361-6.

Haas, C., 2004. Airborne EM sea-ice thickness profiling over brackish Baltic sea water.

Haapala, J.J., Ronkainen, I., Schmelzer, N., Sztobryn, M., 2015. Recent change—sea ice. In: The BACC II Author Team (Ed.), Second Assessment of Climate Change for the Baltic Sea Basin. Regional Climate Studies. Springer, Cham.

HELCOM, 2018a. State of the Baltic Sea – Second HELCOM Holistic Assessment 2011–2016. Baltic Sea Environment Proceedings, p. 155.

HELCOM, 2018b. Diatom/Dinoflagellate Index. HELCOM Pre-core Indicator Report. Online.

HELCOM, 2021. HELCOM Baltic Sea Action Plan.

Hordoir, R., Meier, H.E.M., 2012. Effect of climate change on the thermal stratification of the Baltic Sea: a sensitivity experiment. Climate Dynam. 38, 1703–1713. https://doi.org/10.1007/s00382-011-1036-y.

Kari, E., Merkouriadi, I., Walve, J., Leppäranta, M., Kratzer, S., 2018. Development of under-ice stratification in Himmerfjärden bay, North-Western Baltic proper, and their effect on the phytoplankton spring bloom. J. Mar. Syst. 186, 85–95. https://doi.org/10.1016/j.jmarsys.2018.05.007.

Katlein, C., Arndt, S., Nicolaus, M., Perovich, D.K., Jakuba, M.V., Suman, S., Boetius, A., 2015. Influence of ice thickness and surface properties on light transmission through Arctic Sea ice. J. Geophys. Res. Oceans. 120, 5932–5944. https://doi.org/10.1002/2015JC011018.

Kemp, W.M., Brooks, M.T., Hood, R.R., 2001. Nutrient enrichment, habitat variability and trophic transfer efficiency in simple models of pelagic ecosystems. Mar. Ecol. Prog. Ser. 223, 73–87. https://doi.org/10.3354/meps223073.

Klais, R., Tamminen, T., Kremp, A., Spilling, K., Olli, K., 2011. Decadal-scale changes of dinoflagellates and diatoms in the anomalous Baltic Sea spring bloom. PloS One 6, e21567. https://doi.org/10.1371/journal.pone.0021567.

Klais, R., Tamminen, T., Kremp, A., Spilling, K., An, B.W., Hajdu, S., Olli, K., 2013. Spring phytoplankton communities shaped by interannual weather variability and dispersal limitation: mechanisms of climate change effects on key coastal primary producers. Limnol. Oceanogr. 58, 753–762. https://doi.org/10.4319/lo.2013.58.2.0753.

Kuliński, K., Rehder, G., Asmala, E., Bartosova, A., Carstensen, J., Gustafsson, B., Hall, P. O.J., Humborg, C., Jilbert, T., Jürgens, K., Meier, H.E.M., Müller-Karulis, B., Naumann, M., Olesen, J.E., Savchuk, O., Schramm, A., Slomp, C.P., Sofiev, M., Sobek, A., Szymczycha, B., Undeman, E., 2022. Biogeochemical functioning of the Baltic Sea. Earth Syst. Dynam. 13, 633–685. https://doi.org/10.5194/esd-13-633-2022.

Lehmann, A., Myrberg, K., Post, P., Chubarenko, I., Dailidiene, I., Hinrichsen, H.H., Hüssy, K., Liblik, T., Meier, H.M., Lips, U., Bukanova, T., 2022. Salinity dynamics of the Baltic Sea. Earth Syst. Dynam. 13, 373–392. https://doi.org/10.5194/esd-13-373-2022.

Leppäranta, Myrberg, 2009. Physical Oceanography of the Baltic SeaSpringer-Praxis. Heidelberg, Germany.

Lessin, G., Raudsepp, U., Stips, A., 2014a. Modelling the influence of major Baltic inflows on near-bottom conditions at the entrance of the Gulf of Finland. PloS One 9, e112881. https://doi.org/10.1371/journal.pone.0112881.

Lessin, G., Raudsepp, U., Maljutenko, I., Laanemets, J., Passenko, J., Jaanus, A., 2014b. Model study on present and future eutrophication and nitrogen fixation in the Gulf of Finland, Baltic Sea. J. Mar. Syst. 129, 76–85. https://doi.org/10.1016/j.jmarsys.2013.06.001.

Macias, D., Piroddi, C., Miladinova-Marinova, S., Garcia-Gorriz, E., Friedland, R., Parn, O., Stips, A., 2018. JRC Marine Modelling Framework in Support of the Marine Strategy Framework Directive: Inventory of Models, Basin Configurations and datasets. Update 2018, EUR 29452 EN. Publications Office of the European Union, Luxembourg.

Meier, H.E.M., Kniebusch, M., Dieterich, C., Gröger, M., Zorita, E., Elmgren, R., Myrberg, K., Ahola, M.P., Bartosova, A., Bonsdorff, E., Börgel, F., Capell, R., Carlén, I., Carlund, T., Carstensen, J., Christensen, O.B., Dierschke, V., Frauen, C., Frederiksen, M., Gaget, E., Galatius, A., Haapala, J.J., Halkka, A., Hugelius, G., Hünicke, B., Jaagus, J., Jüssi, M., Käyhkö, J., Kirchner, N., Kjellström, E., Kulinski, K., Lehmann, A., Lindström, G., May, W., Miller, P.A., Mohrholz, V., Müller-Karulis, B., Pavón-Jordán, D., Quante, M., Reckermann, M., Rutgersson, A., Savchuk, O.P., Stendel, M., Tuomi, L., Viitasalo, M., Weisse, R., Zhang, W., 2022. Climate change in the Baltic Sea region: a summary. Earth Syst. Dynam. 13, 457–593. https://doi.org/10.5194/esd-13-457-2022.

Meier, H.E.M., Reckermann, M., Langner, J., Smith, B., Didenkulova, I., 2023. Overview: the Baltic earth assessment reports (BEAR). Earth Syst. Dynam. 14, 519–531. https://doi.org/10.5194/esd-14-519-2023.

Mitra, A., 2006. A multi-nutrient model for the description of stoichiometric modulation of predation in micro- and mesozooplankton. J. Plankton Res. 28, 597–611. https://doi.org/10.1093/plankt/fbi144.
Neumann, T., Schernewski, G., 2008. Eutrophication in the Baltic Sea and shifts in nitrogen fixation analyzed with a 3D ecosystem model. J. Mar. Syst. 74 (1–2), 592–602. https://doi.org/10.1016/j.jmarsys.2008.05.003.
Ojaveer, H., Kotta, J., Outinen, O., Einberg, H., Zaiko, A., Lehtiniemi, M., 2021. Meta-analysis on the ecological impacts of widely spread non-indigenous species in the Baltic Sea. Sci. Total Environ. 786, 147375. https://doi.org/10.1016/j.scitotenv.2021.147375.
Omstedt, A., Humborg, C., Pempkowiak, J., Perttilä, M., Rutgersson, A., Schneider, B., Smith, B., 2014. Biogeochemical control of the coupled CO2-O2 system of the Baltic Sea: a review of the results of Baltic-C. Ambio 43, 49–59. https://doi.org/10.1007/s13280-013-0485-4.
Pärn, O., Friedland, R., Garcia Gorriz, E., Stips, A., 2020. Report on the Biogeochemical Model Setup for the Baltic Sea and Its Applications. EUR 30252 EN. Publications Office of the European Union, Luxembourg.
Pärn, O., Lessin, G., Stips, A., 2021. Effects of sea ice and wind speed on phytoplankton spring bloom in central and southern Baltic Sea. PloS One 16, e0242637. https://doi.org/10.1371/journal.pone.0242637.
Pärn, O., Friedland, R., Rjazin, J., Stips, A., 2022. Regime shift in sea-ice characteristics and impact on the spring bloom in the Baltic Sea. Oceanologia 64, 312–326. https://doi.org/10.1016/j.oceano.2021.12.004.
Pärn, O., Polimene, L., Stips, A., 2024. Evidencing the Impact of Sea Ice on Eutrophication in the Baltic Sea Using New Eutrophication Indicators. Abstract. International Baltic Earth Secretariat Publication No. 23, May 2024, p. 168. ISSN 2198-4247. International Baltic Earth Secretariat Helmholtz-Zentrum Hereon GmbH Max-Planck-Str. 1 D-21502 Geesthacht, Germany.
Polimene, L., Mitra, A., Sailley, S.F., Ciavatta, S., Widdicombe, C.E., Atkinson, A., Allen, J.I., 2015. Decrease in diatom palatability contributes to bloom formation in the western English Channel. Prog. Oceanogr. 137, 484–497. https://doi.org/10.1016/j.pocean.2015.04.026.
Polimene, L., Parn, O., Garcia-Gorriz, E., Macias, D., Stips, A., Duteil, O., Ferreira-Cordeiro, N., Miladinova, S., Piroddi, C., Serpetti, N., 2023. Should we reconsider how to assess eutrophication? J. Plankton Res. 45, 413–420. https://doi.org/10.1093/plankt/fbad022.
Reckermann, M., Omstedt, A., Soomere, T., Aigars, J., Akhtar, N., Bełdowska, M., Bełdowski, J., Cronin, T., Czub, M., Eero, M., Hyytiäinen, K.P., Jalkanen, J.-P., Kiessling, A., Kjellström, E., Kuliński, K., Larsén, X.G., McCrackin, M., Meier, H.E.M., Oberbeckmann, S., Parnell, K., Pons-Seres de Brauwer, C., Poska, A., Saarinen, J., Szymczycha, B., Undeman, E., Wörman, A., Zorita, E., 2022. Human impacts and their interactions in the Baltic Sea region. Earth Syst. Dynam. 13, 1–80. https://doi.org/10.5194/esd-13-1-2022.
Rjazin, J., Alari, V., Pärn, O., 2017. Classifying the ice seasons 1982-2016 using the weighted ice days number as a new winter severity characteristic. EUREKA Phys. Eng. 5, 49–56. https://doi.org/10.21303/2461-4262.2017.00364.
Roman, M.R., Adolf, H.A., Landry, M.R., Madin, L.P., Steinberg, D.K., Zhang, X., 2001. Estimates of oceanic mesozooplankton production: a comparison using the Bermuda and Hawaii time-series data. Deep-Sea Res. II Top. Stud. Oceanogr. 49 (1–3), 175–192. https://doi.org/10.1016/S0967-0645(01)00099-6.
Savchuk, O.P., 2018. Large-scale nutrient dynamics in the Baltic Sea, 1970-2016. Front. Mar. Sci. 5, 95. https://doi.org/10.3389/fmars.2018.00095.
Schmoker, C., Hernandez-Leon, S., Calbet, A., 2013. Microzooplankton grazing in the oceans: impacts, data variability, knowledge gaps and future directions. J. Plankton Res. 35, 691–706. https://doi.org/10.1093/plankt/fbt023.
Siitam, L., Sipelgas, L., Pärn, O., Uiboupin, R., 2017. Statistical characterisation of the sea ice extent during different winter scenarios in the Gulf of Riga (Baltic Sea) using optical remote-sensing imagery. Int. J. Remote Sens. 38, 617–638. https://doi.org/10.1080/01431161.2016.1268734.
Spilling, K., 2007. On the ecology of cold-water phytoplankton in the Baltic Sea. PhD thesis. University of Helsinki. W. & A. de Nottbeck Foundation. Sci. Rep. 31, 1–59.
Spilling, K., Markager, S., 2008. Ecophysiological growth characteristics and modeling of the onset of the spring bloom in the Baltic Sea. J. Mar. Syst. 73, 323–337. https://doi.org/10.1016/j.jmarsys.2006.10.012.
Spilling, K., Olli, K., Lehtoranta, J., Kremp, A., Tedesco, L., Tamelander, T., Klais, R., Peltonen, H., Tamminen, T., 2018. Shifting diatom-dinoflagellate dominance during spring bloom in the Baltic Sea and its potential effects on biogeochemical cycling. Front. Mar. Sci. 5, 327. https://doi.org/10.3389/fmars.2018.00327.
Stigebrandt, A., Andersson, A., 2020. The eutrophication of the Baltic Sea has been boosted and perpetuated by a major internal phosphorus source. Front. Mar. Sci. 7, 572994. https://doi.org/10.3389/fmars.2020.572994.
Stips, A., Bolding, K., Pohlmann, T., Burchard, H., 2004. Simulating the temporal and spatial dynamics of the North Sea using the new model GETM (general estuarine transport model). Ocean Dyn. 54, 266–283. https://doi.org/10.1007/s10236-004-0098-3.
Stoecker, Diane, Pierson, James, July 2019. Predation on protozoa: its importance to zooplankton revisited. J. Plankton Res. 41 (4), 367–373. https://doi.org/10.1093/plankt/fbz027.
Tomczak, M.T., MüllerKarulis, B., Blenckner, T., Ehrnsten, E., Eero, M., Gustafsson, B., Norkko, A., Otto, S.A., Timmermann, K., Humborg, C., 2021. Reference state, structure, regime shifts, and regulatory drivers in a coastal sea over the last century: the Central Baltic Sea case. Limnol. Oceanogr. 67, S266–S284. https://doi.org/10.1002/lno.11975.
Tomczak, M.T., Müller-Karulis, B., Blenckner, T., Ehrnsten, E., Eero, M., Gustafsson, B., Norkko, A., Otto, S.A., Timmermann, K., Humborg, C., 2022. Reference state, structure, regime shifts, and regulatory drivers in a coastal sea over the last century: The Central Baltic Sea case. Limnol. Oceanogr. 67, S266–S284.
Tubay, J.M., Ito, H., Uehara, T., Kakishima, S., Morita, S., Togashi, T., Tainaka, K., Niraula, M.P., et al., 2013. The paradox of enrichment in phytoplankton by induced competitive interactions. Sci. Rep. 3. https://doi.org/10.1038/srep02835.
Vigouroux, G., Kari, E., Beltrán-Abaunza, J.M., Uotila, P., Yuan, D., Destouni, G., 2021. Trend correlations for coastal eutrophication and its main local and whole-sea drivers–application to the Baltic Sea. Sci. Total Environ. 779, 146367. https://doi.org/10.1016/j.scitotenv.2021.146367.
Vihma, T., Haapala, J., 2009. Geophysics of sea ice in the Baltic Sea: a review. Prog. Oceanogr. 80, 129–148. https://doi.org/10.1016/j.pocean.2009.03.006.
Viitasalo, M., Bonsdorff, E., 2022. Global climate change and the Baltic Sea ecosystem: direct and indirect effects on species, communities and ecosystem functioning. Earth Syst. Dynam. 13, 711–747. https://doi.org/10.5194/esd-13-711-2022.
Wasmund, N., 2017. The diatom/dinoflagellate index as an indicator of ecosystem changes in the Baltic Sea. 2. Historical data for use in determination of good environmental status. Front. Mar. Sci. 4, 153. https://doi.org/10.3389/fmars.2017.00153.
Wasmund, N., Kownacka, J., Göbel, J., Jaanus, A., Johansen, M., Jurgensone, I., Lehtinen, S., Powilleit, M., 2017. The diatom/dinoflagellate index as an indicator of ecosystem changes in the Baltic Sea 1. Principle and handling instruction. Front. Mar. Sci. 4, 22. https://doi.org/10.3389/fmars.2017.00022.
Zalewska, T., Wilman, B., Łapeta, B., Marosz, M., Biernacik, D., Wochna, A., Saniewski, M., Grajewska, A., Iwaniak, M., 2024. Seawater temperature changes in the southern Baltic Sea (1959–2019) forced by climate change. Oceanologia 66 (1), 37–55. https://doi.org/10.1016/j.oceano.2023.08.001.
Zeileis, A., Kleiber, C., Krämer, W., Hornik, K., 2003. Testing and dating of structural changes in practice. Comput. Sta.t Data Anal. 44 (1–2), 109–123.